

Diffusion-DRF: Free, Rich, and Differentiable Reward for Video Diffusion Fine-Tuning

Yifan Wang^{1,2}, Yanyu Li², Gordon Guocheng Qian^{2†}, Sergey Tulyakov²
Yun Fu¹, and Anil Kag²

¹Northeastern University ²Snap Inc.

<https://snap-research.github.io/diffusion-drf/>



Fig. 1: Text-to-video fine-tuning with Diffusion-DRF. Our method (bottom row) enhances both text-video alignment (left) and physical fidelity (right), enabling more reliable generation under challenging prompts.

Abstract. Video diffusion alignment has been heavily relied on scalar rewards. These rewards are typically derived from learned reward models in human preference datasets, requiring additional training and extensive collection. Moreover, scalar rewards provide coarse, global supervision, offering limited prompt-generation mismatch credit assignment and making models prone to reward exploitation and unstable optimization. We propose **Diffusion-DRF**, a free, rich, and differentiable reward framework for video diffusion fine-tuning. Diffusion-DRF employs a frozen, off-the-shelf Vision-Language Model (VLM) as the critic, eliminating the need for reward model training. Instead of relying on a single scalar reward, it decomposes each user prompt into multi-dimensional questions with freeform dense VQA explanation queries, yielding information-rich feedback. By direct differentiable optimization over this rich feedback, Diffusion-DRF achieves stable reward-based tuning without preference datasets collection. Diffusion-DRF achieves significant gains both quantitatively and qualitatively, outperforming state-of-the-art Flow-GRPO by 4.74% in overall performance on unseen VBench-2.0.

Keywords: Alignment Fine-tuning · Text-to-Video Generation · Diffusion

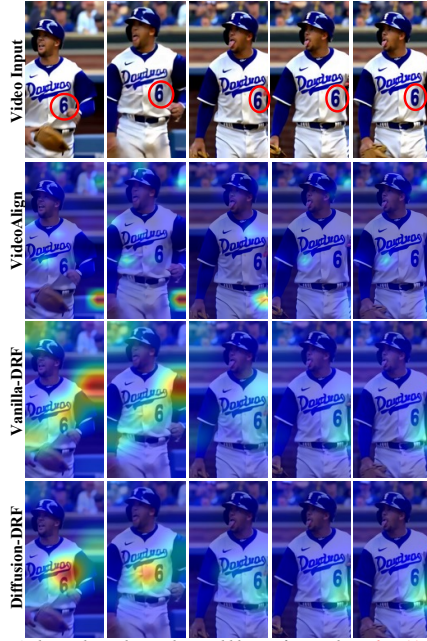
[†] Corresponding author

1 Introduction

Recent advances in diffusion-based text-to-video generation [18, 19, 25, 38, 47, 52] have markedly improved fidelity, temporal coherence, and prompt adherence. Beyond architecture and scaling, a second wave of progress has come from post-training, inspired by alignment practices in LLMs [28, 31, 34, 48] and text-to-image diffusion [7, 11, 14, 36]. The core motivation is to use preference-driven objectives to steer pretrained generators toward human-preferred behaviors that maximum-likelihood training does not capture well. Accordingly, a growing set of post-training methods, such as preference optimization (e.g., DPO-style objectives [22, 42, 43]), reinforcement learning with human or AI feedback [21, 44, 50], and other reward-driven refinements [30, 49], have received increasing attentions to align model outputs with human judgments. Despite these gains, most pipelines still rely on *hand-labeled*, *scalar* preference signals, either from a separate reward models or large-scale DPO-style pairwise annotations.

Such supervision is easily exploited due to its limited scalar supervision and label-intensive, often resulting in reward hacking, training instability, or even policy collapse.

Effective supervision should provide *token-level prompt-generation mismatch credit assignment, indicating where and when generated content mismatches the input prompt*. Such structured feedback, rather than a single scalar signal, enables more stable gradient propagation and mitigates reward hacking or training collapse. However, prior reward tuning approaches [21, 22, 30, 49] typically produce a single scalar score for an entire video. This global supervision fails to distinguish localized spatial or temporal text-video inconsistencies, allowing reinforcement learning updates to under-penalize misaligned regions while over-rewarding globally correlated artifacts. This imbalance often leads to reward exploitation and suboptimal optimization dynamics. To better understand the limitation, we conduct a gradient-level analysis of the recent scalar-reward model VideoAlign [22]. Shown in Fig. 2, their gradients are spatially



A player, dressed in a white and blue uniform with number 66 ...

Fig. 2: Gradient Analysis. In contrast to the latest scalar-based VideoAlign [22] and our Vanilla-DRF baseline built on a simple yes/no text-video alignment VLM feedback, our Diffusion-DRF leverages free and rich structured feedback to yield more semantically coherent and spatially localized gradients, accurately highlighting regions where the generated video violates the input prompt.

diffuse and frequently misplaced, failing to provide precise mismatch credit assignment.

Interestingly, we observe that a pretrained Vision-Language Model (VLM) [1], owing to its strong generalization capability, already serves as a powerful visual quality assessor. Even a simple scalar yes or no alignment signal derived from a frozen VLM forms a strong differentiable reward baseline, which we denote as **Vanilla-DRF**. Despite its simplicity, Vanilla-DRF produces substantially more localized token-level gradients that better indicate where video content deviates from the prompt. Empirically, this basic VLM-based reward already surpasses the latest prior method, VideoAlign, by a significant margin (Fig. 2). However, Vanilla-DRF remains inherently limited by its scalar nature, which can lead to noisy supervision and susceptibility to reward exploitation.

To address these limitations, we propose **Diffusion-DRF, a free, rich, and differentiable reward flow framework** that leverages a frozen, off-the-shelf VLM to fine-tune video diffusion models. We design an automatic prompting pipeline that elicits structured multi-dimensional feedback. Specifically, each prompt is decomposed into multiple targeted questions assessing text-video alignment, visual quality, and physical plausibility, producing binary signals across distinct alignment dimensions, complemented by freeform VQA-style explanations for dense contextual grounding. Together, these responses form *fine-grained, multi-dimensional supervision that is substantially denser and less prone to exploitation than conventional scalar rewards*. This formulation provides the most precise temporally localized learning signals (Fig. 2 row 4) that improve training stability and mitigate reward hacking (see Sec. 4.3), while eliminating the need for additional reward model training or large-scale preference annotation, resulting in a lightweight and extensible alignment pipeline.

Our contributions are summarized as follows:

- We propose **Diffusion-DRF**, a free, rich, and differentiable reward framework for video diffusion fine-tuning. Diffusion-DRF employs a frozen, off-the-shelf VLM as a training-free critic, eliminating the need for reward model training or preference dataset collection.
- We design an automatic annotation pipeline that decomposes each prompt into multiple targeted questions with binary responses, complemented by freeform VQA explanations. This produces multi-dimensional, information-rich feedback that yields temporally and token-aware gradients, substantially improving stability and reducing reward hacking.
- Extensive experiments demonstrate that Diffusion-DRF achieves stable reward-based tuning under both single-prompt and large-scale settings, consistently improving generation quality and outperforming state-of-the-art methods including Flow-GRPO by 4.74% on VBench-2.0.

2 Related Works

Diffusion Model Post-training. Recent progress in LLM post-training [2, 27, 32] has been adapted to visual generation to further improve output qual-

Table 1: Comparisons across reward tuning methods. ✓ indicates preferred. In “Rich Feedback” column, our method is marked with three ✓ to reflect substantially denser supervision via multi-dimensional queries and free-form explanations, whereas VADER [30] and DenseDPO [42] only provide (multiple) scalar feedback signals.

Method	Preference Data Free	Reward-model Training Free	Rich Feedback
VADER [30], InstructVideo [49] Flow-DPO [22], Flow-GRPO [21] DenseDPO [42]	✓		✓
Diffusion-DRF (Ours)	✓	✓	✓✓✓

ity. Existing approaches can generally be divided into two paradigms: reinforcement learning-based optimization and differentiable reward optimization. RL-based methods optimize generators using preference supervision through policy-style updates. Among them, Direct Preference Optimization (DPO) [32] and Group Relative Policy Optimization (GRPO) [34] have become popular choices, as they optimize preference signals through policy-style updates. These methods have been widely explored in both image [15, 37, 45, 53] and video generation [6, 21, 22, 42, 43]. In parallel, differentiable-based approaches update generators using gradients derived from a reward model, enabling end-to-end optimization through the generation process [10, 30, 39, 43, 49]. Despite notable perceptual improvements, existing approaches typically rely on reward models trained from human preference data, which are annotation-intensive, narrow in coverage, and inherently biased. Moreover, these rewards are usually scalar, providing only sparse and coarse supervision. As a consequence, optimization can lead to reward hacking and unstable updates. These limitations have motivated follow-up efforts toward richer and more fine-grained feedback [20], but such approaches require even more extensive data collection. Check the comparisons of our Diffusion-DRF with previous arts in Tab. 1.

Learning from AI Feedback Recent advancements have demonstrated that Vision–Language Models (VLMs) can transcend simple image-text matching to perform complex tasks such as aesthetic assessment, fine-grained grounding, and compositional reasoning. Thus, VLMs have functioned as automated oracles capable of judging various dimensions of visual quality which are widely used in different T2I/T2V tasks such as data selection [4, 5, 26, 35, 40] and evaluation [9, 12, 13, 51]. In particular, [3] uses VLM as a zero-shot reward model to quantify prompt–image alignment within a reinforcement learning framework. [8] leverages Gemini-generated preference data to perform DPO fine-tuning. [24] uses VLM as a differentiable scalar reward to improve multimodal control. Despite these advances, directly optimizing video diffusion models with differentiable VLM feedback remains non-trivial and largely unexplored.

3 Method

Given a text prompt c , a video diffusion model $v_\theta(\mathbf{z}_t \mid c)$ generates a video latent \mathbf{z}_0 through iterative denoising from Gaussian noise \mathbf{z}_T in latent space,

where T denotes the total number of diffusion steps. Our goal is to fine-tune the pretrained model v_θ using feedback derived from a reward function $f(\mathbf{v}, c)$, where \mathbf{v} denotes the predicted clean video in pixel space decoded from \mathbf{z}_0 .

Diffusion-DRF leverages a frozen, off-the-shelf Vision-Language Model (VLM) as a training-free critic, without learning a separate reward model or collecting preference pairs. We first introduce a minimal formulation, **Vanilla-DRF**, with a single binary reward in Sec. 3.1. We then extend it to our proposed structured multi-dimensional rich reward formulation in Sec. 3.2, and finally introduce our automatic annotation pipeline in Sec. 3.3.

3.1 Vanilla-DRF: Single Binary Differentiable Reward

Vanilla-DRF is a minimal formulation of Diffusion-DRF, which also provides free and differentiable VLM feedback without reward model training. The difference is Vanilla-DRF relies on simple single binary reward.

Single Binary Reward. As a minimal formulation, we query the VLM with a single binary question: “Does this video match the prompt?” The VLM produces logits y over **Yes** and **No**.

Logit-level Reward. We define a differentiable reward using the log-probability:

$$R_{\text{vanilla}}(\mathbf{v}, c) = \log p(y | \mathbf{v}, c), \quad (1)$$

Truncated Backpropagation Through Diffusion. Let $\mathbf{z}_T \rightarrow \dots \rightarrow \mathbf{z}_0$ denote the full denoising trajectory in training. We truncate gradients at step $T-K$ by applying a stop-gradient operator to \mathbf{z}_{T-K} , and backpropagate only through the final K updates:

$$\nabla_{\theta} R_{\text{vanilla}} = \frac{\partial R}{\partial \mathbf{v}} \frac{\partial \mathbf{v}}{\partial \mathbf{z}_0} \sum_{k=1}^K \frac{\partial \mathbf{z}_{k-1}}{\partial \theta}, \quad \mathbf{z}_K \leftarrow \text{sg}(\mathbf{z}_K), \quad (2)$$

Here $\text{sg}(\cdot)$ denotes the stop-gradient operator, which treats \mathbf{z}_{T-K} as constant with respect to θ . As a result, gradients flow only through the last K denoising steps for optimized memory efficiency (see *Appendix* for ablation).

Limitation of Vanilla-DRF. A single global binary judgment compresses multiple factors, including entity presence, motion correctness, interaction consistency, into one scalar signal. Such supervision is inherently sparse. Because the model is only encouraged to increase an overall **Yes** score, it may exploit superficial cues that correlate with the prompt while neglecting specific semantic or physical requirements. This makes the reward easy to game and provides weak guidance for identifying which component of the generation should be corrected, often leading to unstable or misaligned gradient updates. See Sec. 4 for results.

3.2 Diffusion-DRF: Multi-Dimensional Rich Differentiable Reward

The single binary reward in Vanilla-DRF provides a global scalar signal that entangles multiple failure modes. To obtain structured and harder-to-exploit supervision, we extend the formulation to multi-dimensional rich feedback formed

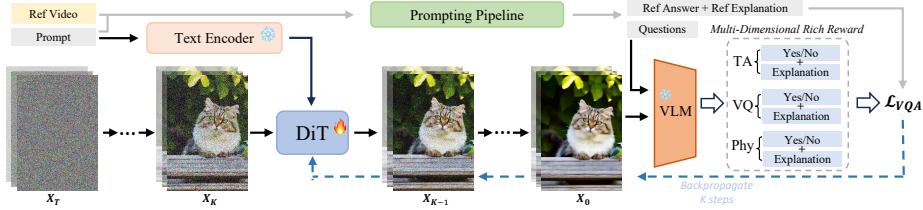


Fig. 3: Pipeline of Diffusion-DRF. Given a reference video and its caption as the prompt, our Diffusion-DRF framework queries a frozen VLM with structured multi-dimensional questions spanning text-video alignment (TA), physical fidelity (Phy), and visual quality (VQ). For each dimension, the VLM produces a Yes/No binary judgment together with a dense free-form explanation. The logit difference through next-token prediction defines a differentiable reward for each query, and the aggregated multi-dimensional rewards are backpropagated through the VAE decoder and the final K denoising steps to update the latent diffusion model (e.g., DiT [29]).

by a set of targeted binary queries derived from explicit semantic and physical decompositions with their corresponding freeform dense explanations.

Structured Query Set. Given a prompt c , we automatically construct a set of sub-questions for distinct dimension:

$$\mathcal{Q}(c) = \{q_i(c)\}_{i=1}^N,$$

where each q_i probes a specific and localized aspect of the generation. The query set is organized along three complementary dimensions in our implementation:

- *Text-Video Alignment (TA)*: semantic entities, attributes, actions, and interactions explicitly described in c ;
- *Physical Fidelity (Phy)*: motion realism and physical plausibility;
- *Visual Quality (VQ)*: perceptual fidelity including sharpness, artifacts, texture preservation, and exposure stability.

Each query q_i is instantiated as a minimal Yes/No question followed by an extra query of *free-form explanation*. The VLM is prompted to first produce a binary decision token and then generate a dense textual rationale describing where and why the video succeeds or fails for that specific dimension.

Reference-Guided Queries. For physical fidelity (Phy) and visual quality (VQ), we adopt a reference-guided evaluation mechanism. Given a caption-matched real video \mathbf{v}^{ref} , the VLM evaluates the generated video \mathbf{v} contrastively:

$$f(\mathbf{v}, \mathbf{v}^{\text{ref}}, q_i),$$

where the reference clip provides a physical and perceptual anchor. This stabilizes assessment of motion realism, interaction plausibility, and appearance statistics by grounding the judgment in realistic dynamics and textures.

Free, Rich, and Differentiable Rewards. For each query q_i , the frozen VLM generates a token sequence

$$y_i = (y_i^0, y_i^1, \dots, y_i^{(L)}),$$

where the first token $y_i^0 \in \{\text{Yes}, \text{No}\}$ represents the binary judgment, and the remaining tokens form a dense free-form explanation, where $L = 512$ represents the maximum number of response tokens. This constrained format enforces localized judgments while preserving rich diagnostic information.

Diffusion-DRF Training Objective is defined as the summed log-likelihood over all generated tokens:

$$\mathcal{L}_{\text{VQA}} = - \sum_{i=1}^N \sum_{t=1}^{L_i} \log p_{\phi} \left(y_i^{(t)} \mid \mathbf{c}_i, y_i^{(<t)} \right), \quad (3)$$

where the conditioning context \mathbf{c}_i is defined as

$$\mathbf{c}_i = \begin{cases} (\mathbf{v}, q_i), & q_i \in \text{TA}, \\ (\mathbf{v}, \mathbf{v}^{\text{ref}}, q_i), & q_i \in \{\text{Phy}, \text{VQ}\}, \end{cases}$$

and p_{ϕ} denotes the frozen VLM next-token distribution.

This objective aggregates token-level supervision across structured queries spanning text-video alignment (TA), physical fidelity (Phy), and visual quality (VQ). By jointly optimizing the binary decisions and their corresponding explanations through next-token prediction, the model receives structured and localized gradients for each semantic and physical facet. Unlike a single global judgment, this multi-dimensional formulation decomposes supervision into interpretable components, improving credit assignment and mitigating shortcut exploitation. *Overall, our Diffusion-DRF framework is training-free with respect to reward modeling, provides rich multi-dimensional feedback, and remains fully differentiable through the VLM next-token objective, forming a free, rich, and differentiable reward tuning paradigm.*

3.3 Automatic Annotation Pipeline

To enable the multi-dimensional supervision described above, we require structured annotations that decompose each video data into explicit semantic and physical facets. We construct such annotations automatically through a lightweight parsing and prompting pipeline, as illustrated in Fig. 4.

Shown in Fig. 4 “Decompositions”, given a video caption as the prompt, we first decompose it into atomic scene elements in text, including background environment, objects, humans, attributes, spatial relations, and their interactions. This decomposition identifies the explicit entities and behaviors that should appear in the video. The extracted components are then incorporated into the formulation of one structured Yes/No question for each supervision dimension shown in “Questions”. Each dimension therefore produces one Yes/No judgment accompanied by a dense free-form explanation that references the decomposed components. The decomposed entities and interactions are also embedded directly into both the question wording and the expected explanations (Fig. 4 “Reference Answers”), ensuring that the VLM grounds its judgment in concrete semantic and physical details.

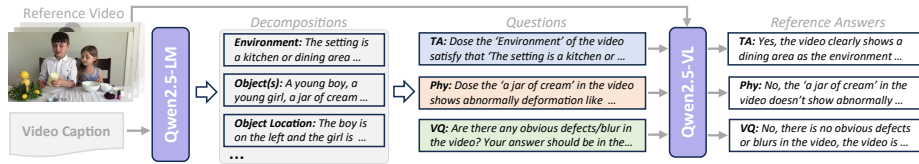


Fig. 4: Automate Annotation Pipeline. Instead of relying on vague global questions or human preference pairs, we construct structured queries directly from captioned videos. Given a video caption as the prompt, we extract atomic key points and formulate targeted questions across three domains: text-video alignment (TA), physical fidelity (Phy), and visual quality (VQ). Each question is posed in a minimal and unambiguous Yes/No format with a constrained free-form explanation, encouraging precise and localized judgments from the frozen VLM. For Phy and VQ, the same queries are additionally applied to caption-matched ground-truth videos to obtain reference answers that anchor physical and perceptual assessment. Detailed prompt templates and domain facets are provided in *Appendix*.

This automated annotation pipeline replaces vague global evaluation with rich, grounded, aspect-aware supervision. It requires only captioned videos, avoids reward model training and human preference collection, and scales naturally to large datasets. By injecting explicit semantic and physical elements into both the question and explanation, the resulting feedback becomes more informative, interpretable, and stable for diffusion fine-tuning.

4 Experiments

4.1 Experimental Setup

Training Details. We apply Diffusion-DRF to the pretrained Wan2.1-1.3B-T2V [38] with Qwen2.5-VL-7B [1] as the default VLM. We only train the DiT and freeze other components (VAE, text-encoder, and VLM). Videos are generated at 512×288 resolution with 49 frames under 25 denoise steps during training and 30 steps at inference. AdamW [16, 23] optimizer is used with a learning rate of $1e^{-5}$, 32 A100 80GB GPUs, and batch size 1 per GPU. The training is conducted on 5K high-quality captioned videos from OpenVid-1M [26]. See *Appendix* for the sampling procedure. Automatic annotation pipeline is by Qwen2.5-7B.

Efficiency Optimization. Back-propagating VLM feedback through the full diffusion chain is prohibitively memory-intensive, as both the DiT denoiser and the frozen VLM are multi-billion parameter models with large activation footprints. A naive implementation quickly exceeds GPU VRAM limits. To make differentiable reward flow practically feasible, we design a set of optimizations:

- *Efficient Video Decoding.* Instead of using the original heavy decoder, we trained an efficient H3AE VAE decoder following [41] that reproduces the similar level decoding quality with a lighter backbone and employ it during Diffusion-DRF, achieving 24.3% less memory consumption in decoding.

Table 2: Quantitative results on VBench-2.0. In addition to the overall score, we report representative sub-dimension metrics closely related to text-video alignment and physical fidelity. The best results are highlighted in **bold**, and the second best are underlined. For completeness, we evaluate Diffusion-DRF with three different VLM backbones: InternVL3-1B [54], Qwen2.5-VL-3B, and Qwen2.5-VL-7B [1], denoted as Diffusion-DRF (1B), (3B), and (7B), respectively. All methods are trained with Wan2.1-1.3B-T2V as base model on the same datasets for fair comparisons.

Method	VBench-2.0										
	Overall	Creativity	Common Sense	Controllability	Human Fidelity	Physics	Material	Dynamic Attribute	Motion Rationality	Complex Landscape	Cameras Motion
Wan2.1-1.3B-T2V [38]	52.99	53.79	55.52	26.59	80.65	48.40	36.23	37.00	37.36	17.33	20.68
Flow-DPO [22]	50.27	46.77	50.28	<u>27.76</u>	71.76	54.78	69.24	40.29	35.06	<u>18.44</u>	22.24
Flow-GRPO [21]	50.64	44.71	50.85	25.48	77.80	54.37	69.07	36.63	36.21	14.89	19.32
PickScore [17]	49.62	35.97	55.23	23.88	81.89	51.13	66.67	39.19	36.78	16.89	22.84
VideoAlign [22]	53.55	49.64	56.09	26.32	<u>81.43</u>	54.26	65.26	41.76	37.93	<u>18.44</u>	23.15
Vanilla-DRF (7B)	53.70	52.70	54.66	26.64	78.55	55.61	65.31	36.63	36.21	16.67	19.44
Diffusion-DRF (1B)	53.10	50.85	56.90	24.33	77.31	<u>56.21</u>	68.63	40.30	40.20	15.11	28.40
Diffusion-DRF (3B)	<u>53.72</u>	<u>53.93</u>	57.53	25.95	76.74	54.42	<u>70.00</u>	<u>42.49</u>	41.38	18.22	23.15
Diffusion-DRF (7B)	55.38	54.58	<u>56.96</u>	27.98	80.51	56.85	75.82	42.86	<u>40.23</u>	21.56	<u>24.69</u>

- *Frame Subsampling.* To further control VLM activation growth with video length, we uniformly subsample frames before feeding them to the VLM. In practice, we sample 10 frames from the generated video and 10 reference frames from a caption-matched real video, which preserves semantic coverage while substantially reducing memory usage (see *Appendix* for ablation).
- *Denoising Aware Activation Checkpointing.* We apply gradient checkpointing across diffusion steps to trade additional computation for lower memory usage. Concretely, we retain only the input latent at each denoising step and re-compute intermediate DiT activations during the backward pass. This avoids storing the full denoising trajectory in memory, enabling stable end-to-end gradient propagation through the diffusion chain.
- *Truncated Back-propagation.* While checkpointing allows backpropagation through the entire sampling chain, we find that truncating the backward pass to the last K sampling steps (see Eq. (2)) substantially improves optimization speed and overall performance. Refer to *Appendix* for ablation.

Baselines. We compare Diffusion-DRF to reinforcement learning based methods Flow-DPO [22] and Flow-GRPO [21]. For differentiable reward tuning approaches, we compare to PickScore [17] and VideoAlign [22]. All methods fine-tune the same Wan2.1-1.3B-T2V [38] as the base model on the same dataset for fair comparisons. We evaluate the checkpoints of different training steps and report the best result for each model.

Evaluation. We evaluate text-to-video performance on VBench-2.0 [51] that provides 1,013 prompts covering advanced aspects from human actions to physical phenomena. It aggregates 18 sub-dimensions into five axes: *creativity, commonsense, controllability, human fidelity, and physics*. We also use the VideoGenEval prompt set [46], which includes 400 instruction-heavy prompts designed to stress text–video alignment. For this set, we adopt a pairwise preference protocol: for each prompt, we generate videos from competing models and use VideoAlign [22] to evaluate video quality to indicate which model is preferred.

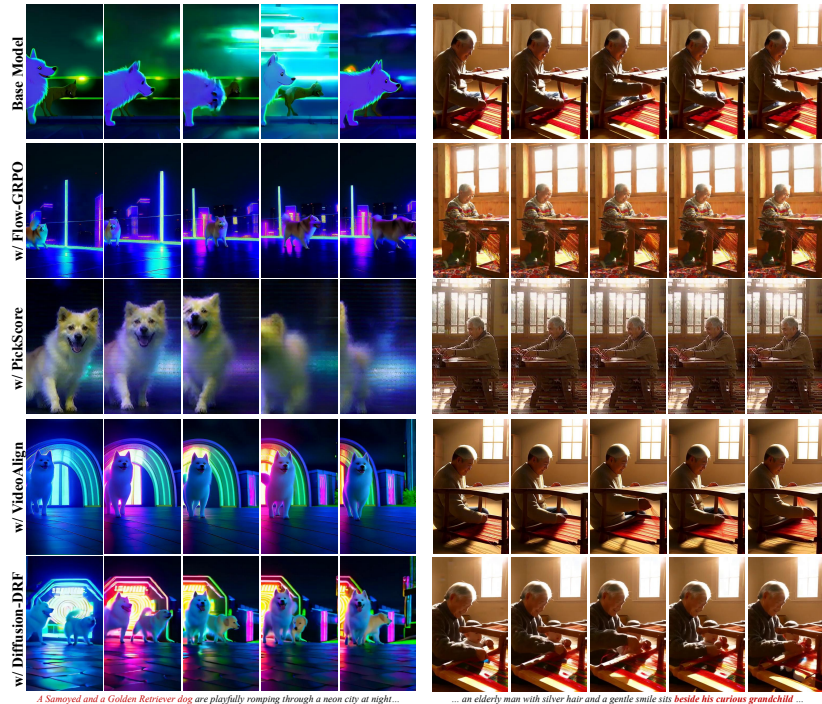


Fig. 5: Qualitative Comparison. All videos are generated under the same configuration and random seed. The pre-trained model, Flow-GRPO, and the model fine-tuned with VideoAlign all fail to align with the text descriptions. The model trained with PickScore exhibits significant degradation in video quality. Only our model successfully generates videos that accurately satisfy the prompt requirements. In the left example, only our method produces a video with two dogs with more accurate lighting applied. On the right, only our method correctly generates the grandchild beside the elderly man. See supplementary videos for full video comparisons across methods.

4.2 Main Results

Quantitative results on VBench-2.0. As shown in Table 2, Diffusion-DRF improves the base model across nearly all dimensions with different frozen VLM as reward models. The gains are particularly pronounced on *Dynamic Attribute* and *Physics*, reflecting better adherence to complex prompts and stronger physical plausibility. Particularly, scaling the reward model from 1B to 7B yields additional improvements, consistent with the stronger feedback provided by a better VLM. Compared to state-of-the-art reinforcement learning tuning methods Flow-DPO [22] and Flow-GRPO [21], our approach consistently improves performance as indicated in “Overall” score and achieves much higher quality in “Creativity”, “Common Sense”, “Materials”, “Dynamic Attributes”, “Motion Rationality”, and “Complex Landscape”, demonstrating a better prompt following.

Compared with state-of-the-art differentiable reward approaches that rely on training dedicated reward models, such as PickScore [17] and VideoAlign [22],

our method leverages a frozen VLM and achieves consistently stronger ‘‘Overall’’ performance. In practice, these customized reward models are often susceptible to reward hacking, exhibiting biases toward particular visual styles, for example overly flashy human-centric illustrations, which ultimately harms creativity and controllability. Our approach, without reward model training, delivers clear improvements on these dimensions as well as ‘‘Physics’’, ‘‘Creativity’’, and ‘‘Common Sense’’ metrics.

Pair-wise metric on VideoGen-Eval. To further substantiate the gains, we conduct a pair-wise evaluation with a video reward model trained on human-preference data.

For each caption, we generate two videos with the same configure and score them by VideoAlign [22]. Fig. 6 reports win / tie / loss rates for two comparisons: (i) Base vs. Diffusion-DRF and (ii)

	Base model wins	Ties	Flow-GRPO wins	Diffusion-DRF wins
TA	40.7%	12.3%	47.0%	38.0%
VQ	30.3%	20.0%	49.5%	20.3%
MQ	20.0%	42.5%	37.5%	22.5%
OA	35.7%	11.0%	53.3%	32.3%

Fig. 6: Pair-wise evaluation on VideoGen-Eval.

With the same prompt and configuration, we perform pairwise comparisons of generated videos using the VideoAlign scores of text-video alignment (TA), visual quality (VQ), motion quality (MQ) and overall (OA). We compare the Diffusion-DRF with the base model (left) and the Flow-GRPO (right) respectively. Beyond the aggregate win rate, we observe that the advantage persists across all major dimensions, indicating that the improvements are not confined to a single aspect of generation.

Human Evaluation. We also conducted a blind pairwise comparison between the base model and our method by human annotators on text-video alignment perspective which we addressed. We used 200 random prompt samples from the VideoGen-Eval set. As shown in the Tab. 3, Diffusion-DRF achieved a 29% win rate on text-video alignment (TA) over the base model, demonstrating significant improvements in human-perceived quality.

Table 3: Human evaluation on text-video alignment of Diffusion-DRF vs. the base model.

Win (%)	Tie (%)	Lose (%)
29.0	54.0	17.0

Qualitative results. We present qualitative comparisons in Fig. 5, where all videos are generated using the same noise seed to ensure direct and fair evaluation. Diffusion-DRF substantially improves generation quality over the base model, producing videos with stronger semantic fidelity and visual coherence. Compared with the reinforcement learning based Flow-GRPO [21] and models trained with other differentiable reward models, including VideoAlign [22] and PickScore [17], our Diffusion-DRF demonstrates more reliable text-video alignment. For example, competing methods fail to correctly model two different dogs under complex lighting in the left case and omit the child in the right case, whereas our approach faithfully captures both the described motion and entities.

4.3 In-depth Analysis of Diffusion-DRF

Training dynamics analysis. We track model performance across training steps to examine how different reward formulations affect optimization stability. As shown in Fig. 7, we record the VBench-2.0 ‘Overall’ score over an extended training horizon. *Notably, Diffusion-DRF is the only method whose performance consistently remains above the base model throughout the entire training process.* In contrast, the model trained with PickScore [17] deteriorates at an early stage, quickly dropping significantly below the base model, indicating clear reward hacking. VideoAlign [22] improves in the early phase but gradually declines afterward, again suggesting reward exploitation. A similar pattern is observed with Vanilla-DRF, where a single scalar reward also leads to instability and performance degradation. These observations indicate that existing learned or scalar reward formulations fail to provide robust and stable supervisory signals during optimization.

A likely explanation is that fine-tuning a foundation model into a narrow reward predictor or a scalar reward weakens its general video understanding, causing it to prioritize superficial cues instead of the holistic behaviors we aim to improve. In contrast, Diffusion-DRF keeps the VLM frozen to preserve its general video understanding capacity and leverages multi-dimensional rich feedback to provide structured supervision that is harder to exploit.

Gradient visualization. Similar to Sec. 1, we further analyze the gradients induced by different reward formulations. Gradients directly determine the optimization direction. The activated regions in a gradient heatmap correspond to the parts of the video that the reward signal considers most responsible for the mismatch with the prompt. In other words, correctly localized gradient activation indicates that the reward provides semantically aligned corrective signals. We visualize and compare the gradient distributions produced by customized reward VideoAlign [22], Vanilla-DRF, Diffusion-DRF

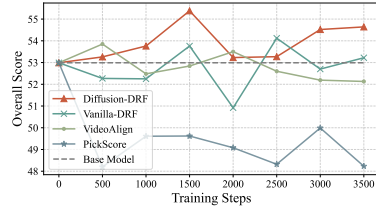


Fig. 7: Training dynamics of the same base model optimized with different rewards. VBench-2.0 Overall score over training steps is provided. Diffusion-DRF is the only method that maintains consistently higher performance than the base model throughout training, demonstrating substantially more robust optimization dynamics than others.

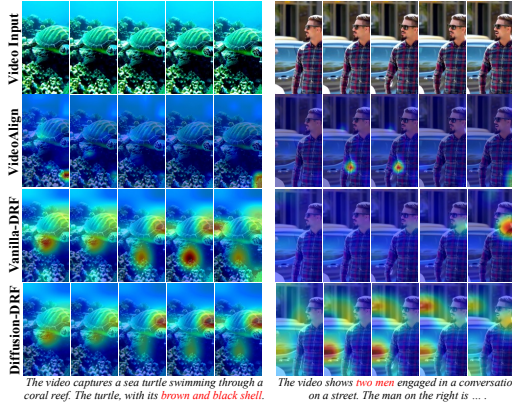


Fig. 8: Gradient heatmap visualizations for different reward formulations. Original video failed to satisfy the color requirement of the turtle’s shell (left) and two men (right).

and Diffusion-DRF. As illustrated in Fig. 8, when fine-grained details are missing or incorrectly rendered, *only Diffusion-DRF produces spatially localized gradients that precisely highlight the regions requiring modification*. In contrast, customized reward models [22] trained on narrow preference data often produce diffuse or misplaced gradient signals, reflecting shortcut correlations or dataset bias, compared to ours that use a frozen VLM, a general large-scaled trained critic. Similarly, without multi-dimensional rich feedback, a single global reward query in Vanilla-DRF can entangle multiple semantic factors, leading to ambiguous optimization signals. As a result, the activated regions do not consistently correspond to the true source of error in the generated video.

Single-Prompt Reward Tuning. Sec. 4.2 demonstrates that Diffusion-DRF

consistently outperforms prior reward tuning approaches. To provide a more controlled and intuitive comparison, similar to DreamBooth [33], which fine-tunes a base model on a single concept, *we introduce a single-prompt reward tuning setting*, where the model parameters are optimized using only one prompt under the guidance of a reward model. This controlled setting allows us to more directly examine whether a reward model can provide effective supervision. Shown in Fig. 9, when the base model fails to generate a satisfactory video, learned reward models such as PickScore [17] and VideoAlign [22] fail to deliver informative signals about where

and how the generation is incorrect, leading to clear overfitting: the generated videos show significant style shift or noticeable visual distortions, where the text-video alignment remains low.

4.4 Ablation Study

Effect of multi-dimensional feedback is studied by using different combinations of TA, VQ, and Phy. Using TA alone degrades the overall score of the base model, suggesting that alignment-only supervision is more susceptible to reward exploitation. Adding Phy only increases the Physics metric but harms perceptual quality, indicating over-optimization toward a single property. In contrast, TA+VQ improves the overall score, showing that explicit visual quality supervision stabilizes generation. Finally, combining TA+VQ+Phy achieves the



Fig. 9: Qualitative results of single-prompt reward tuning. Under the same configuration and noise seed, we fine-tune the generator on a single prompt for 100 steps. The base model, VideoAlign [22], and PickScore [17] all exhibit noticeable defects. Specifically, the base model fails to render “pink bowl”. Model fine-tuned with VideoAlign loses “red tomatos” and changes the overall style. PickScore fails to preserve “pink bowl” and distorts arms. In contrast, Diffusion-DRF produces the most faithful result without introducing visual distortions.

Table 4: Ablation studies on question sets and styles.

Method	VBench-2.0					
	Overall	Creativity	Common Sense	Controllability	Human Fidelity	Physics
Baseline	52.99	53.79	55.52	26.59	80.65	48.40
TA	52.15	49.41	53.80	27.03	74.88	55.64
TA + Phy	53.55	50.56	60.12	25.72	75.57	<u>55.78</u>
TA + VQ	53.92	<u>52.34</u>	55.81	<u>27.80</u>	79.02	54.65
TA + VQ + Phy	55.38	54.58	<u>56.96</u>	27.98	<u>80.51</u>	56.85
Binary question (w/o explanation)	53.55	50.56	60.12	25.72	75.57	55.78
Explanation w/ CoT	54.25	52.75	58.11	26.52	79.80	56.09

best performance, improving both physical plausibility and perceptual realism. These results suggest that multi-dimensional questions provide complementary constraints that prevent reward hacking and guide balanced optimization.

Effect of explanation. We study the role of free-form explanations through two ablations: (1) removing the explanation and keeping only binary questions; and (2) varying the length of the reference explanations used for supervision. When only binary questions are used, the feedback becomes significantly less informative, resulting in weaker optimization and degraded performance, as shown in Tab. 4 “Binary question (w/o explanation)”. This confirms that binary signals alone provide limited guidance for correcting fine-grained errors. We further analyze the impact of explanation length. By default, we use reference explanations with an average length of 50 tokens. We then adopt Chain-of-Thought (CoT) prompting to generate detailed reference explanations (denoted as “Explanation w/ CoT” in the table). Incorporating CoT-style explanations can improve performance further. See *Appendix* for more discussion of CoT.

5 Conclusion

We introduced **Diffusion-DRF**, a video diffusion post-training framework with free, rich, and differentiable VLM-guided reward optimization. Instead of relying on coarse scalar preferences that are typically narrow in scope and require extensive human annotation, our approach extracts logit-level feedback from a frozen VLM and backpropagates it through the diffusion process as localized gradients. Our multi-dimensional feedback pipeline spanning text-video alignment, physical fidelity, and visual quality inspection provides structured, fine-grained supervision, while the complementary free-form explanations further supply dense corrective signals, together making the optimization substantially harder to exploit. Combined with a set of efficiency optimizations, including efficient video decoding, frame subsampling, denoising aware activation checkpointing, and truncated backpropagation Diffusion-DRF maintains strong mismatch credit assignment while reducing computational burden. Extensive experiments demonstrate consistent gains of Diffusion-DRF in prompt adherence, physical plausibility, and perceptual quality, while revealing the limitations of state-of-the-art reward models. Requiring neither reward model training nor large-scale preference data, and being empirically less prone to reward hacking due to its rich multi-dimensional feedback, Diffusion-DRF offers a practical and scalable solution for aligning diffusion-based video generation models.

References

1. Bai, S., Chen, K., Liu, X., Wang, J., Ge, W., Song, S., Dang, K., Wang, P., Wang, S., Tang, J., Zhong, H., Zhu, Y., Yang, M., Li, Z., Wan, J., Wang, P., Ding, W., Fu, Z., Xu, Y., Ye, J., Zhang, X., Xie, T., Cheng, Z., Zhang, H., Yang, Z., Xu, H., Lin, J.: Qwen2.5-VL technical report. arXiv preprint arXiv:2502.13923 (2025)
2. Bai, Y., Kadavath, S., Kundu, S., Askell, A., Kernion, J., Jones, A., Chen, A., Goldie, A., Mirhoseini, A., McKinnon, C., Chen, C., Olsson, C., Olah, C., Hernandez, D., Drain, D., Ganguli, D., Li, D., Tran-Johnson, E., Perez, E., Kerr, J., Mueller, J., Ladish, J., Landau, J., Ndousse, K., Lukosuite, K., Lovitt, L., Sellitto, M., Elhage, N., Schiefer, N., Mercado, N., DasSarma, N., Lasenby, R., Larson, R., Ringer, S., Johnston, S., Kravec, S., Showk, S.E., Fort, S., Lanham, T., Telleen-Lawton, T., Conerly, T., Henighan, T., Hume, T., Bowman, S.R., Hatfield-Dodds, Z., Mann, B., Amodei, D., Joseph, N., McCandlish, S., Brown, T., Kaplan, J.: Constitutional ai: Harmlessness from ai feedback. arXiv preprint arXiv:2212.08073 (2022)
3. Black, K., Janner, M., Du, Y., Kostrikov, I., Levine, S.: Training diffusion models with reinforcement learning. arXiv preprint arXiv:2305.13301 (2023)
4. Chen, L., Wei, X., Li, J., Dong, X., Zhang, P., Zang, Y., Chen, Z., Duan, H., Lin, B., Tang, Z., Yuan, L., Qiao, Y., Lin, D., Zhao, F., Wang, J.: Sharegpt4video: Improving video understanding and generation with better captions. *Advances in Neural Information Processing Systems* **37**, 19472–19495 (2024)
5. Chen, T.S., Siarohin, A., Menapace, W., Deyneka, E., wei Chao, H., Jeon, B.E., Fang, Y., Lee, H.Y., Ren, J., Yang, M.H., Tulyakov, S.: Panda-70m: Captioning 70m videos with multiple cross-modality teachers (2024), <https://arxiv.org/abs/2402.19479>
6. Cheng, G., Yang, D., Huang, Z., Si, J., Si, C., Liu, Z.: Realdpo: Real or not real, that is the preference. arXiv preprint arXiv:2510.14955 (2025)
7. Fan, Y., Watkins, O., Du, Y., Liu, H., Ryu, M., Boutilier, C., Abbeel, P., Ghavamzadeh, M., Lee, K., Lee, K.: DPOK: Reinforcement learning for fine-tuning text-to-image diffusion models. *NeurIPS* (2023)
8. Furuta, H., Zen, H., Schuurmans, D., Faust, A., Matsuo, Y., Liang, P., Yang, S.: Improving dynamic object interactions in text-to-video generation with ai feedback. arXiv preprint arXiv:2412.02617 (2024)
9. Ghosh, D., Hajishirzi, H., Schmidt, L.: Geneval: An object-focused framework for evaluating text-to-image alignment. *Advances in Neural Information Processing Systems* **36**, 52132–52152 (2023)
10. He, X., Jiang, D., Zhang, G., Ku, M., Soni, A., Siu, S., Chen, H., Chandra, A., Jiang, Z., Arulraj, A., Wang, K., Do, Q.D., Ni, Y., Lyu, B., Narsupalli, Y., Fan, R., Lyu, Z., Lin, Y., Chen, W.: VideoScore: Building automatic metrics to simulate fine-grained human feedback for video generation. In: *EMNLP* (2024)
11. Hong, J., Paul, S., Lee, N., Rasul, K., Thorne, J., Jeong, J.: Margin-aware preference optimization for aligning diffusion models without reference. In: *ICLR Workshop* (2025)
12. Hu, Y., Liu, B., Kasai, J., Wang, Y., Ostendorf, M., Krishna, R., Smith, N.A.: Tifa: Accurate and interpretable text-to-image faithfulness evaluation with question answering. In: *Proceedings of the IEEE/CVF International Conference on Computer Vision*. pp. 20406–20417 (2023)
13. Huang, Z., He, Y., Yu, J., Zhang, F., Si, C., Jiang, Y., Zhang, Y., Wu, T., Jin, Q., Chanpaisit, N., Wang, Y., Chen, X., Wang, L., Lin, D., Qiao, Y., Liu, Z.: VBench: Comprehensive benchmark suite for video generative models. In: *CVPR* (2024)

14. Karthik, S., Coskun, H., Akata, Z., Tulyakov, S., Ren, J., Kag, A.: Scalable ranked preference optimization for text-to-image generation. arXiv preprint arXiv:2410.18013 (2024)
15. Karthik, S., Coskun, H., Akata, Z., Tulyakov, S., Ren, J., Kag, A.: Scalable ranked preference optimization for text-to-image generation. In: Proceedings of the IEEE/CVF International Conference on Computer Vision. pp. 18399–18410 (2025)
16. Kingma, D.P., Ba, J.: Adam: A method for stochastic optimization. arXiv preprint arXiv:1412.6980 (2014)
17. Kirstain, Y., Polyak, A., Singer, U., Matiana, S., Penna, J., Levy, O.: Pick-a-Pic: An open dataset of user preferences for text-to-image generation. NeurIPS (2023)
18. Kong, W., Tian, Q., Zhang, Z., Min, R., Dai, Z., Zhou, J., Xiong, J., Li, X., Wu, B., Zhang, J., Wu, K., Lin, Q., Yuan, J., Long, Y., Wang, A., Wang, A., Li, C., Huang, D., Yang, F., Tan, H., Wang, H., Song, J., Bai, J., Wu, J., Xue, J., Wang, J., Wang, K., Liu, M., Li, P., Li, S., Wang, W., Yu, W., Deng, X., Li, Y., Chen, Y., Cui, Y., Peng, Y., Yu, Z., He, Z., Xu, Z., Zhou, Z., Xu, Z., Tao, Y., Lu, Q., Liu, S., Zhou, D., Wang, H., Yang, Y., Wang, D., Liu, Y., Jiang, J., Zhong, C.: HunyuanVideo: A systematic framework for large video generative models. arXiv preprint arXiv:2412.03603 (2024)
19. Li, J., Long, Q., Zheng, J., Gao, X., Piramuthu, R., Chen, W., Wang, W.Y.: T2V-Turbo-v2: Enhancing video generation model post-training through data, reward, and conditional guidance design. In: ICLR (2025)
20. Liang, Y., He, J., Li, G., Li, P., Klimovskiy, A., Carolan, N., Sun, J., Pont-Tuset, J., Young, S., Yang, F., Ke, J., Dvijotham, K.D., Collins, K., Luo, Y., Li, Y., Kohlhoff, K.J., Ramachandran, D., Navalpakkam, V.: Rich human feedback for text-to-image generation. In: CVPR (2024)
21. Liu, J., Liu, G., Liang, J., Li, Y., Liu, J., Wang, X., Wan, P., Zhang, D., Ouyang, W.: Flow-GRPO: Training flow matching models via online rl. arXiv preprint arXiv:2505.05470 (2025)
22. Liu, J., Liu, G., Liang, J., Yuan, Z., Liu, X., Zheng, M., Wu, X., Wang, Q., Qin, W., Xia, M., Wang, X., Liu, X., Yang, F., Wan, P., Zhang, D., Gai, K., Yang, Y., Ouyang, W.: Improving video generation with human feedback. arXiv preprint arXiv:2501.13918 (2025)
23. Loshchilov, I., Hutter, F.: Decoupled weight decay regularization. In: ICLR (2019)
24. Luo, G., Granskog, J., Holynski, A., Darrell, T.: Dual-process image generation. arXiv preprint arXiv:2506.01955 (2025)
25. Menapace, W., Siarohin, A., Skorokhodov, I., Deyneka, E., Chen, T.S., Kag, A., Fang, Y., Stoliar, A., Ricci, E., Ren, J., Tulyakov, S.: Snap video: Scaled spatiotemporal transformers for text-to-video synthesis. CVPR (2024)
26. Nan, K., Xie, R., Zhou, P., Fan, T., Yang, Z., Chen, Z., Li, X., Yang, J., Tai, Y.: Openvid-1m: A large-scale high-quality dataset for text-to-video generation. arXiv preprint arXiv:2407.02371 (2024)
27. Ouyang, L., Wu, J., Jiang, X., Almeida, D., Wainwright, C.L., Mishkin, P., Zhang, C., Agarwal, S., Slama, K., Ray, A., Schulman, J., Hilton, J., Kelton, F., Miller, L., Simens, M., Askill, A., Welinder, P., Christiano, P., Leike, J., Lowe, R.: Training language models to follow instructions with human feedback. In: Advances in Neural Information Processing Systems (NeurIPS) (2022), https://proceedings.neurips.cc/paper_files/paper/2022/file/b1efde53be364a73914f58805a001731-Paper-Conference.pdf

28. Ouyang, L., Wu, J., Jiang, X., Almeida, D., Wainwright, C., Mishkin, P., Zhang, C., Agarwal, S., Slama, K., Ray, A., Schulman, J., Hilton, J., Kelton, F., Miller, L., Simens, M., Aspell, A., Welinder, P., Christiano, P.F., Leike, J., Lowe, R.: Training language models to follow instructions with human feedback. In: *NeurIPS (2022)*
29. Peebles, W., Xie, S.: Scalable diffusion models with transformers. *ICCV (2023)*
30. Prabhudesai, M., Mendonca, R., Qin, Z., Fragkiadaki, K., Pathak, D.: Video diffusion alignment via reward gradients. *arXiv preprint arXiv:2407.08737 (2024)*
31. Rafailov, R., Sharma, A., Mitchell, E., Manning, C.D., Ermon, S., Finn, C.: Direct Preference Optimization: Your language model is secretly a reward model. *NeurIPS (2023)*
32. Rafailov, R., Sharma, A., Mitchell, E., Manning, C.D., Ermon, S., Finn, C.: Direct preference optimization: Your language model is secretly a reward model. *Advances in neural information processing systems* **36**, 53728–53741 (2023)
33. Ruiz, N., Li, Y., Jampani, V., Pritch, Y., Rubinstein, M., Aberman, K.: Dreambooth: Fine tuning text-to-image diffusion models for subject-driven generation. In: *CVPR (2023)*
34. Shao, Z., Wang, P., Zhu, Q., Xu, R., Song, J., Bi, X., Zhang, H., Zhang, M., Li, Y.K., Wu, Y., Guo, D.: Deepseekmath: Pushing the limits of mathematical reasoning in open language models. *arXiv preprint arXiv:2402.03300 (2024)*
35. Sun, J., Fu, D., Hu, Y., Wang, S., Rassin, R., Juan, D.C., Alon, D., Herrmann, C., Van Steenkiste, S., Krishna, R., et al.: Dreamsync: Aligning text-to-image generation with image understanding feedback. In: *Proceedings of the 2025 Conference of the Nations of the Americas Chapter of the Association for Computational Linguistics: Human Language Technologies (Volume 1: Long Papers)*. pp. 5920–5945 (2025)
36. Wallace, B., Dang, M., Rafailov, R., Zhou, L., Lou, A., Purushwalkam, S., Ermon, S., Xiong, C., Joty, S., Naik, N.: Diffusion model alignment using direct preference optimization. In: *CVPR (2024)*
37. Wallace, B., Dang, M., Rafailov, R., Zhou, L., Lou, A., Purushwalkam, S., Ermon, S., Xiong, C., Joty, S., Naik, N.: Diffusion model alignment using direct preference optimization. In: *Proceedings of the IEEE/CVF Conference on Computer Vision and Pattern Recognition*. pp. 8228–8238 (2024)
38. Wan, T., Wang, A., Ai, B., Wen, B., Mao, C., Xie, C.W., Chen, D., Yu, F., Zhao, H., Yang, J., Zeng, J., Wang, J., Zhang, J., Zhou, J., Wang, J., Chen, J., Zhu, K., Zhao, K., Yan, K., Huang, L., Feng, M., Zhang, N., Li, P., Wu, P., Chu, R., Feng, R., Zhang, S., Sun, S., Fang, T., Wang, T., Gui, T., Weng, T., Shen, T., Lin, W., Wang, W., Wang, W., Zhou, W., Wang, W., Shen, W., Yu, W., Shi, X., Huang, X., Xu, X., Kou, Y., Lv, Y., Li, Y., Liu, Y., Wang, Y., Zhang, Y., Huang, Y., Li, Y., Wu, Y., Liu, Y., Pan, Y., Zheng, Y., Hong, Y., Shi, Y., Feng, Y., Jiang, Z., Han, Z., Wu, Z.F., Liu, Z.: Wan: Open and advanced large-scale video generative models. *arXiv preprint arXiv:2503.20314 (2025)*
39. Wang, Y., Tan, Z., Wang, J., Yang, X., Jin, C., Li, H.: LiFT: Leveraging human feedback for text-to-video model alignment. *arXiv preprint arXiv:2412.04814 (2024)*
40. Wu, X., Huang, S., Wang, G., Xiong, J., Wei, F.: Boosting text-to-video generative model with mllms feedback. *Advances in Neural Information Processing Systems* **37**, 139444–139469 (2024)
41. Wu, Y., Li, Y., Skorokhodov, I., Kag, A., Menapace, W., Girish, S., Siarohin, A., Wang, Y., Tulyakov, S.: H3ae: High compression, high speed, and high quality autoencoder for video diffusion models. *arXiv preprint arXiv:2504.10567 (2025)*

42. Wu, Z., Kag, A., Skorokhodov, I., Menapace, W., Mirzaei, A., Gilitschenski, I., Tulyakov, S., Siarohin, A.: Densedpo: Fine-grained temporal preference optimization for video diffusion models. arXiv preprint arXiv:2506.03517 (2025)
43. Xu, J., Huang, Y., Cheng, J., Yang, Y., Xu, J., Wang, Y., Duan, W., Yang, S., Jin, Q., Li, S., Teng, J., Yang, Z., Zheng, W., Liu, X., Ding, M., Zhang, X., Gu, X., Huang, S., Huang, M., Tang, J., Dong, Y.: VisionReward: Fine-grained multi-dimensional human preference learning for image and video generation. arXiv preprint arXiv:2412.21059 (2024)
44. Xue, Z., Wu, J., Gao, Y., Kong, F., Zhu, L., Chen, M., Liu, Z., Liu, W., Guo, Q., Huang, W., Luo, P.: DanceGRPO: Unleashing grpo on visual generation. arXiv preprint arXiv:2505.07818 (2025)
45. Yang, K., Tao, J., Lyu, J., Ge, C., Chen, J., Shen, W., Zhu, X., Li, X.: Using human feedback to fine-tune diffusion models without any reward model. In: Proceedings of the IEEE/CVF Conference on Computer Vision and Pattern Recognition. pp. 8941–8951 (2024)
46. Yang, Y., Fan, K., Sun, S., Li, H., Zeng, A., Han, F., Zhai, W., Liu, W., Cao, Y., Zha, Z.J.: Videogen-eval: Agent-based system for video generation evaluation. arXiv preprint arXiv:2503.23452 (2025)
47. Yang, Z., Teng, J., Zheng, W., Ding, M., Huang, S., Xu, J., Yang, Y., Hong, W., Zhang, X., Feng, G., Yin, D., Zhang, Y., Wang, W., Cheng, Y., Xu, B., Gu, X., Dong, Y., Tang, J.: CogVideoX: Text-to-video diffusion models with an expert transformer. In: ICLR (2025)
48. Yu, T., Yao, Y., Zhang, H., He, T., Han, Y., Cui, G., Hu, J., Liu, Z., Zheng, H.T., Sun, M., Chua, T.S.: RLHF-V: Towards trustworthy mllms via behavior alignment from fine-grained correctional human feedback. In: CVPR (2024)
49. Yuan, H., Zhang, S., Wang, X., Wei, Y., Feng, T., Pan, Y., Zhang, Y., Liu, Z., Albanie, S., Ni, D.: InstructVideo: Instructing video diffusion models with human feedback. In: CVPR (2024)
50. Zhang, D., Lan, G., Han, D.J., Yao, W., Pan, X., Zhang, H., Li, M., Chen, P., Dong, Y., Brinton, C., Luo, J.: SePPO: Semi-policy preference optimization for diffusion alignment. arXiv preprint arXiv:2410.05255 (2024)
51. Zheng, D., Huang, Z., Liu, H., Zou, K., He, Y., Zhang, F., Gu, L., Zhang, Y., He, J., Zheng, W.S., Qiao, Y., Liu, Z.: Vbench-2.0: Advancing video generation benchmark suite for intrinsic faithfulness. arXiv preprint arXiv:2503.21755 (2025)
52. Zheng, Z., Peng, X., Yang, T., Shen, C., Li, S., Liu, H., Zhou, Y., Li, T., You, Y.: Open-Sora: Democratizing efficient video production for all (March 2024), <https://github.com/hpcaitech/Open-Sora>
53. Zhu, H., Xiao, T., Honavar, V.G.: Dspo: Direct score preference optimization for diffusion model alignment. In: The Thirteenth International Conference on Learning Representations (2025)
54. Zhu, J., Wang, W., Chen, Z., Liu, Z., Ye, S., Gu, L., Tian, H., Duan, Y., Su, W., Shao, J., Gao, Z., Cui, E., Wang, X., Cao, Y., Liu, Y., Wei, X., Zhang, H., Wang, H., Xu, W., Li, H., Wang, J., Deng, N., Li, S., He, Y., Jiang, T., Luo, J., Wang, Y., He, C., Shi, B., Zhang, X., Shao, W., He, J., Xiong, Y., Qu, W., Sun, P., Jiao, P., Lv, H., Wu, L., Zhang, K., Deng, H., Ge, J., Chen, K., Wang, L., Dou, M., Lu, L., Zhu, X., Lu, T., Lin, D., Qiao, Y., Dai, J., Wang, W.: Internvl3: Exploring advanced training and test-time recipes for open-source multimodal models (2025), <https://arxiv.org/abs/2504.10479>

6 Appendix

6.1 Overview

In this supplementary material, Sec. 1.2 details the training and inference configurations, including VAE, text encoder, and scheduler settings ; Sec. 1.3 describes the data sampling procedure using 25k pairs from OpenVid-1M filtered by a prompt pipeline ; Sec. 1.4 presents additional results, including generalization on CogVideoX, training dynamics, and ablation studies on input frames (N_f), gradient truncation length (K), and CoT reasoning; Sec. 1.5 discloses the full prompting configurations for caption decomposition and training evaluations (TA, Phy, VQ) ; and Sec. 1.6 provides further qualitative evidence through single-prompt fine-tuning samples and gradient heatmaps.

6.2 More Training Details

We provide further training and inference details in this section to support reproducibility. Overall, we follow the standard configuration of Wan2.1-1.3B-T2V.

Table 5: Training Configure.

class	config	value
VAE	temporal_compression_ratio	4
	spatial_compression_ratio	8
Text Encoder	tokenizer	google/umt5-xxl
	text_length	512
	vocab_size	256384
	dim	4096
	dim_attn	4096
	dim_ffn	10240
	num_heads	64
	num_layers	24
	num_buckets	32
	shared_pos	False
	dropout	0.0
Scheduler	num_train_timesteps	10000
	shift	5.0
	use_dynamic_shifting	false
	base_shift	0.5
	max_shift	1.15
	base_image_seq_len	256
	max_image_seq_len	4096

6.3 Data Sampling Procedure

We randomly sampled 25k video-caption pairs based on the category distribution in OpenVid-1M. These pairs were then processed by our prompting pipeline to

get the reference answers. To ensure the VLM could correctly understand the video, we retained only the cases where all references were 'yes'. This process resulted in our final dataset.

6.4 Additional Results

Table 6: Additional comparisons. We report the results of Flow-DPO, CogVideoX (CVX), and our methods on VBench-2.0.

Method	VBench-2.0					
	Overall	Creativity	Common Sense	Controllability	Human Fidelity	Physics
CogVideoX	49.52	37.88	54.87	24.56	78.10	52.18
w/ Diffusion-DRF	51.89	40.63	57.75	27.11	81.28	52.69

Additional Quantitative Comparisons We further apply Diffusion-DRF to CogVideoX to evaluate its generalization beyond the main diffusion backbone. As shown in Table 6, Diffusion-DRF consistently improves the base CogVideoX model across all reported dimensions on VBench-2.0, raising the overall score from 49.52 to 51.89. Notably, the gains are not limited to a single aspect: Creativity improves from 37.88 to 40.63, Common Sense from 54.87 to 57.75, Controllability from 24.56 to 27.11, Human Fidelity from 78.10 to 81.28, and Physics from 52.18 to 52.69. These results suggest that the benefit of Diffusion-DRF is backbone-agnostic, and that the proposed differentiable reward can consistently enhance multiple aspects of video generation rather than over-optimizing a narrow subset of metrics.

Additional Ablation Studies Number of input frames (N_f). We further study how the number of video frames fed into the VLM affects training. As shown in Table 7, increasing N_f leads to a clear and consistent improvement in overall performance, with the score rising from 50.83 at $N_f = 2$ to 55.38 at $N_f = 10$. This trend indicates that denser temporal observations help the VLM better understand the video content and provide more informative reward signals. In particular, larger N_f also improves several key dimensions, including Common Sense and Physics, suggesting that richer temporal coverage is especially helpful for reasoning about object dynamics and physical plausibility. However, this benefit comes with a steadily increasing memory cost, as VRAM usage grows from 62 GB to 75 GB. Due to GPU memory constraints, we are unable to further scale up the number of input frames.

Gradient truncation Length (K). We set the number of backpropagation steps K to 4 in the main results and further ablate its effect in Table 7. The results show that using more backpropagation steps consistently improves performance: the overall score increases from 53.16 at $K = 1$ to 55.38 at $K = 4$.

Table 7: Additional ablation studies on input frames. We report the results of the ablations on changing the number of input frames for VLM on VBench-2.0. All model are trained with the same configure shared with the Diffusion-DRF.

Method	VBench-2.0						Training VRAM Usage (Gb)
	Overall	Creativity	Common Sense	Controllability	Human Fidelity	Physics	
$N_f = 2$	50.83	48.43	48.10	27.50	80.96	54.14	62
$N_f = 4$	51.45	43.22	53.51	27.64	78.4	54.45	65
$N_f = 6$	52.19	43.85	55.23	29.25	78.88	53.75	68
$N_f = 8$	54.80	54.50	55.81	28.10	79.61	56.03	71
$N_f = 10$	55.38	54.58	56.96	27.98	80.51	56.85	75
$K = 4$	55.38	54.58	56.96	27.98	80.51	56.85	75
$K = 3$	55.05	52.75	58.11	27.52	80.80	56.09	69
$K = 2$	54.36	52.45	57.24	27.45	78.50	56.18	63
$K = 1$	53.16	52.95	52.93	25.45	79.49	54.99	56
CoT (1K-steps)	54.25	52.75	58.11	26.52	79.80	56.09	75
CoT (2K-steps)	53.31	49.15	57.19	25.84	79.53	55.22	75
CoT (3K-steps)	51.89	43.75	55.81	24.83	79.13	53.92	75
w/o ref frames	53.15	50.41	54.50	27.80	78.88	56.34	72

This suggests that propagating reward gradients through more denoising steps provides stronger and more effective corrective supervision. Nevertheless, larger K also incurs higher training cost and memory overhead, which limits further scaling in practice.

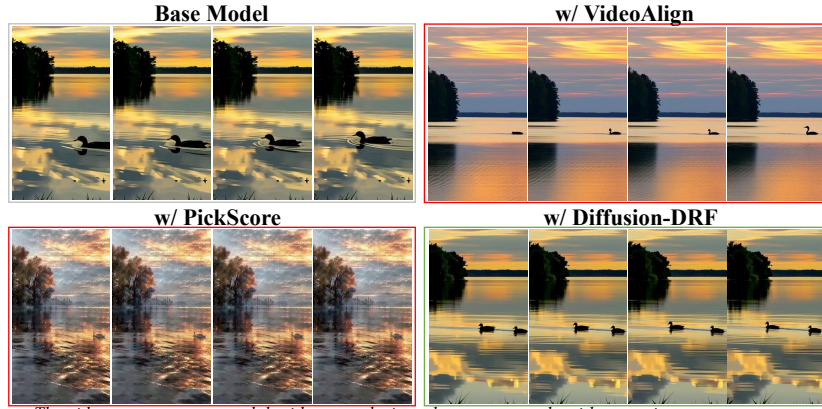
Discussion of CoT answer. We also study the effect of using Chain-of-Thought (CoT) to generate longer explanations. In our method, we explicitly constrain explanations to be shorter than 50 words so that the supervision remains concise and focused. By contrast, CoT-based reference generation typically expands the explanation to over 100 words, introducing much more redundant content. As shown in Table 7, CoT supervision can improve performance at the early stage of training, achieving 54.25 at 1K steps, which suggests that longer explanations initially provide richer diagnostic cues. However, this benefit is short-lived: performance drops to 53.31 at 2K steps and further to 51.89 at 3K steps, indicating substantially earlier collapse than the non-CoT setting. We attribute this to the excessive verbosity of CoT outputs, where many irrelevant tokens dilute useful gradients and amplify optimization noise during training.

6.5 Detailed Prompts

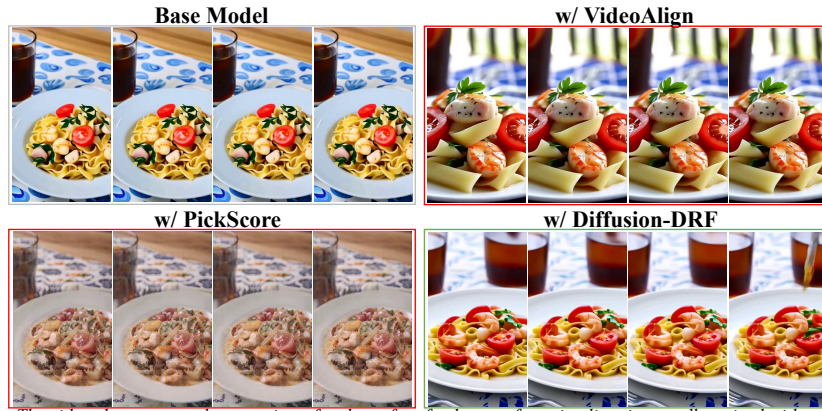
In this section, we present the prompts used in our prompting pipeline (Figs. 13 and 14) as well as the prompts used during training (Figs. 15, 16 and 17), which cover the various facets used for analyzing the generated videos.

6.6 Additional Visual Results

We provide more visual results in the appendix. Fig. 10 shows more examples of single prompt finetuning. Figs. 11 and 12 show further visualization of the gradient heatmaps. We also provide visual results in video format on the project page.



The video captures a serene lakeside scene during what appears to be either sunrise or sunset, *two ducks* are seen across the frame..



The video showcases a close-up view of a plate of seafood pasta, featuring linguine noodles mixed with shrimp, squid, and chunks of chicken. *A fork* is also visible on the left side of the frame.

Fig. 10: Additional Samples of Single Prompt Finetuning.

On the project page, we first present qualitative comparisons among the base model, the model fine-tuned with VideoAlign, and our Diffusion-DRF model. These visual results show that our method improves both text-video alignment and physical fidelity. We also provide examples demonstrating that when the base model already produces high-quality videos, our method preserves these strengths. In contrast, VideoAlign may lead to over-optimization and deteriorate originally high-quality generations. We additionally present single prompt finetuning videos and several cases in which our method performs particularly well.

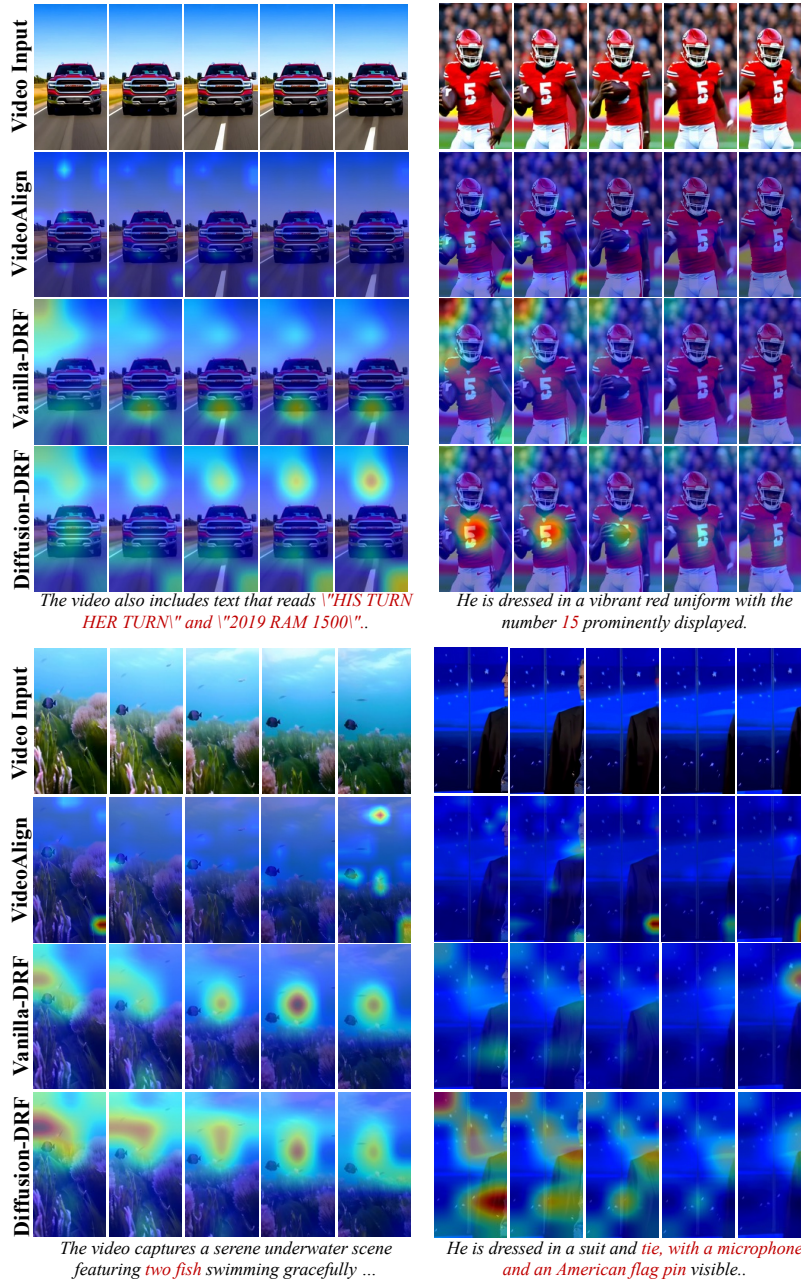


Fig. 11: Additional Gradient Heatmaps - Part1.

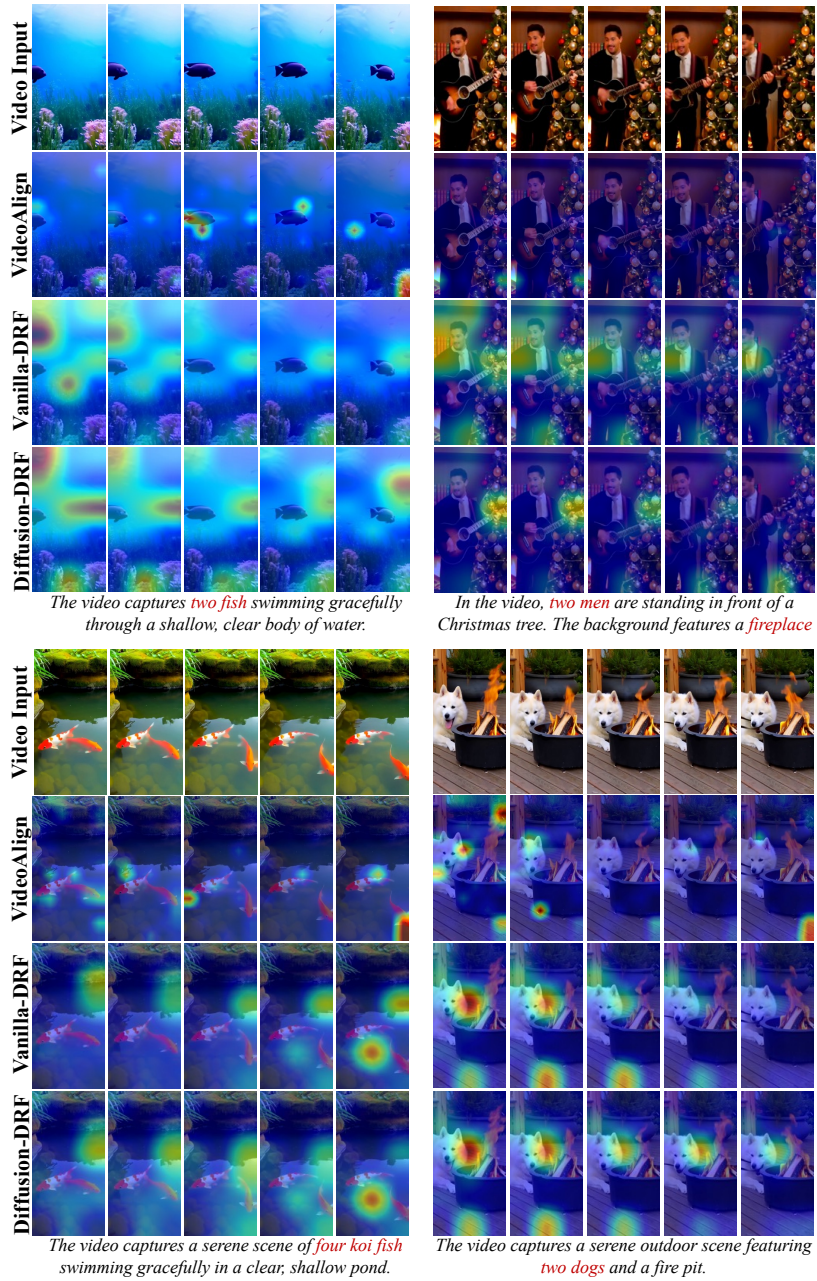


Fig. 12: Additional Gradient Heatmaps - Part2.

Prompts of caption decomposition - Part1:

Please analyze the following video generation prompt by breaking it down based on the following key components:

1. Environment: Describe the overall setting and static elements of the environment.
2. Object(s): List the main objects/entities in the scene.
3. Objects' Motion: Describe how each object moves or interacts within the environment. Include direction, speed, and behavior.
4. Object Location / Spatial Distribution: Describe the spatial layout of objects in the scene. Where are they located (e.g., left/right/center/far/near)? Is the composition symmetrical or unbalanced?
5. Color Requirement: Describe any mentioned or implied colors for objects or environment. Mention the dominant tone or palette.
6. Lighting: Describe the light source(s), brightness, shadows, and general mood (e.g., backlit, dim, dramatic, diffuse sunlight).
7. Letter/Text Presence: Indicate whether there are any textual elements (e.g., signs, billboards), whether text is legible, and how it integrates into the scene.
8. Camera Motion: Describe how the camera moves or stays still (e.g., tracking, panning, zooming, handheld, fixed). Also indicate how this affects perception of the scene. Return the result in a structured bullet-point format, your response of each elements should be as simplified as possible.

Important: Only extract the the element is merely described atmospherically or implicitly observed — only count it if there is a clear instruction or strong implication to generate it.

Here is the prompt to analyze:

{video caption}

The answer format should be in dict format:

"Environment": content, "Object(s)": content, "Object Location/Spatial Distribution": content, "Objects' Motion": content, "Color Requirement": content, "Camera Motion": content

Here is a decomposed example for you:

The video generation prompt is

"a moment on a rainy day in a city. The street, slick with rain, reflects the surrounding buildings and trees, creating a mirror-like surface. Two motorbikes, one blue and the other white, are making their way down this wet road. They are moving towards the camera, their tires kicking up droplets of water. On the left side of the street, several tents and umbrellas have been set up, providing shelter from the rain. These structures add a splash of color to the otherwise gray scene. On the right side of the street, a red and yellow sign stands out, although the text on it is not visible. The sky overhead is a blanket of gray, heavy with rain clouds. Despite the inclement weather, there's a certain tranquility to the scene. It's as if time has slowed down, allowing one to fully take in the details of this rainy day in the city."

Fig. 13: Prompts used for the caption decomposition. Part 1

Prompts of caption decomposition - Part2:
Your answer:
{
‘Environment’: ‘1). A city street during a rainy day. 2). The road is slick with rain, creating a mirror-like reflection of surrounding buildings and trees. 3). The sky is gray and heavy with rain clouds.’

‘Object(s)’: ‘1). Two motorbikes. 2). Several tents and umbrellas. 3). A red and yellow sign (text not visible).’
‘Objects’ Motion’: ‘1). The two motorbikes are moving toward the camera. 2). Their tires are kicking up water droplets from the wet road. 3). Other objects (tents, umbrellas, sign) are static.’
‘Object Location / Spatial Distribution’: ‘1).The motorbikes are on the street. 2). Tents and umbrellas are placed on the left side of the street. 3). The sign is on the right side.’
‘Color Requirement’: ‘1). The overall palette is gray, reflecting the rainy weather. 2). The motorbikes are blue and white. 3). The sign is red and yellow. 4). The tents and umbrellas are colorful.’
‘Lighting:’: ‘Not explicitly stated.’
‘Letter/Text Presence’: ‘Not explicitly stated.’
‘Camera Motion’: ‘Not explicitly stated.’
}

Fig. 14: Prompts used for the caption decomposition - Part2.

Prompts of TA:
Given this AI-generated video, does it successfully fulfill the {key} condition: {description}?
Respond with ‘Yes’ or ‘No’, Answer ‘Yes’ if the video largely matches the description. Answer ‘No’ if the video clearly contradicts the description. The presence of additional elements in the video is acceptable as long as they do not conflict with the core description. Please provide a brief explanation for your answer.
Provide your analysis and explanation in JSON with keys: answer (e.g., Yes or No), explanation.

Fig. 15: Prompts used in the training for text-video alignment (TA).

Prompts of Phy:

You are a careful video forensics assistant. You are given two videos: a test video (the first 10 frames) which is ai-generated and a real video (the last 10 frames). The test video is generated by the caption of the real video. The caption is `{video prompt}`

Your task is evaluating whether the test video shows physics-related defects. You should compare both videos and use the provided caption as high-level intent. Focus on physical plausibility, not style or aesthetics.

You need to analyze it in these aspects:

- Liquid flow irregularity – e.g., non-inertial or discontinuous flow, volume popping, gravity-inconsistent motion, impossible splashes.
- Abnormal object deformation – e.g., rigid objects bending/stretching without cause, topology changes (parts merging/splitting).
- Abnormal texture/material change – e.g., surface turns matte→glossy without cause, texture swimming/flicker detached from geometry.
- Abnormal motion – e.g., inertia/acceleration violations, teleporting, time reversals, jitter not explained by camera motion.
- Unnatural interpenetration – e.g., objects passing through each other or ground, missing collisions/contacts.

If the prompt doesn't have related physical aspects, you should answer 'No'.

Output strictly as JSON with this schema (no extra text):

```
{
  "liquid flow irregularity": "Yes or No",
  "abnormal deformation": "Yes or No",
  "abnormal texture change": "Yes or No",
  "abnormal motion": "Yes or No",
  "unnatural interpenetration": "Yes or No",
}
```

Fig. 16: Prompts used in the training for physical fidelity (Phy).

Prompts of VQ:

Compare the test video (the first 10 frames) to the reference frame (the last 10 frames) and decide if the video shows obvious visual-quality (VQ) defects relative to the reference.

Consider only: blur (defocus/motion), compression artifacts (blocking/ringing/mosquito), noise/grain, banding, flicker, rolling-shutter, aliasing/moire, over-smoothing.

Return ONLY this JSON (no timestamps):

```
{
  "has obvious defect": Yes / No,
  "dominant issue": "none / defocus blur / motion blur / blocking / ringing /
  mosquito noise / grain noise / banding / flicker / rolling shutter / aliasing /
  moire / over or smoothing",
  "evidence": ["short visual cues vs reference, e.g., softer edges than reference",
  block edges visible around text"],
}
```

Rules:

- Compare against the reference frame's look (sharpness, texture, edges, tones).
- Be conservative; if unsure, choose false and note 'uncertain' in evidence."

Fig. 17: Prompts used in the training for visual quality (VQ).